Acute exacerbation of idiopathic pulmonary fibrosis model by small amount of lipopolysaccharide in rats

Hikaru Miyamoto,[1] Shigekazu Takemura,[2,]* Yukiko Minamiyama,[3] Takuma Tsukioka,[1] Michihito Toda,[1] Noritoshi Nishiyama,[1] and Toshihiko Shibata[4]

[1]Department of Thoracic Surgery, [2]Department of Hepato-Biliary-Pancreatic Surgery, and [4]Department of Cardiovascular Surgery, Graduate School of Medicine, Osaka City University, 1-4-3 Asahimachi, Abeno-ku, Osaka 545-8585, Japan
[3]Food Hygiene and Environmental Health Division of Applied Life Science, Graduate School of Life and Environmental Sciences, Kyoto Prefectural University, 1-5 Shimogamo-Hangi-cho, Sakyo-ku, Kyoto 606-8522, Japan

Idiopathic pulmonary fibrosis, a chronic and progressive lung disease with poor prognosis, presents with acute exacerbation. Pathophysiology and treatments for this acute exacerbation, and an appropriate animal model to perform such examinations, have not established yet. We presented a rat model for assessing acute exacerbation in cases of idiopathic pulmonary fibrosis. Wistar rats were intratracheally administered bleomycin (3 mg/kg) to induce pulmonary fibrosis. After 7 days, lipopolysaccharide (0, 0.05, or 0.15 mg/kg) was administered. In the bleomycin or lipopolysaccharide group, there were almost no change in the oxygen partial pressure, arterial blood gas (PaO$_2$), plasma nitrite/nitrate, nitric oxide synthase, and lung nitrotyrosine levels. In the bleomycin (+)/lipopolysaccharide (+) groups, these three indicators deteriorated significantly. The plasma nitrite/nitrate and PaO$_2$ levels were significantly correlated in the bleomycin (+) groups (r = 0.758). Although lung fibrosis was not different with or without lipopolysaccharide in the bleomycin (+) groups, macrophage infiltration was marked in the bleomycin (+)/ lipopolysaccharide (+) group. There were many NOS2-positive macrophages, and the PaO$_2$ levels decrease may be induced by the nitric oxide production of macrophages in the lung. This model may mimic the pathophysiological changes in cases of acute exacerbation during idiopathic pulmonary fibrosis in humans.

Key Words: idiopathic pulmonary fibrosis, acute exacerbation, lipopolysaccharide, bleomycin, Wistar rats

I n recent years, chronic respiratory diseases (CRDs) have become a major global health issue with over one billion cases and more than four million deaths annually.[1] CRDs include chronic obstructive pulmonary disease, asthma, and idiopathic interstitial pneumonia.[1] Particularly, idiopathic pulmonary fibrosis (IPF), the most common form of idiopathic interstitial pneumonia, is a chronic, progressive, and inevitably fatal lung disease with a poor prognosis.

It has been recognized that some patients with IPF experience acute exacerbation (AE). Such cases were first reported in 1993 and were identified as the development of acute lung injury/ acute respiratory distress syndrome (ALI/ARDS).[2] However, the cause and pathophysiology of AE in IPF cases remain unknown, although therapeutic interventions, especially surgical treatments, have been reported to provoke AE of IPF.[3] Furthermore, AE of IPF has a poor outcome with an overall short-term mortality of >50% and 90–100% in patients requiring ventilator assistance.[4] The mortality rates of AE range from 33.3% to 100%, as reported in several studies; however, the results consistently showed poor prognosis associated with AE of IPF.[5–8]

Two antifibrotic therapies, administration of nintedanib and pirfenidone, have been recommended by recent guidelines for the treatment of chronic and stable IPF; however, there are no recommended treatments for AE.[9] In addition, suitable animal models for investigating the pathophysiology of AE of IPF have not yet been established, which was attributed to the multiple causes of ALI/ARDS. Endotoxin is considered to be one of the causes, as it is reported to be significantly involved in the ALI/ ARDS development.[10]

Lipopolysaccharides (LPSs) in the cell walls of gram-negative bacteria are known to induce inflammation and are frequently used to generate animal models of ALI/ARDS.[11–15] In contrast, there are several animal models of IPF induced by the injection of bleomycin (BLM), fluorescein isothiocyanate, or silica. The pulmonary fibrosis animal model induced by the BLM injection is the most characterized animal model in use today.[16] A mouse model combining the two types of injuries has been reported.[17] In this report, the dose of LPS was 0.5 mg/kg, which was approximately the same as that used in other ALI/ARDS animal models.[11,18] This LPS dose could cause severe inflammation in mice. Therefore, this mouse model may be strongly influenced by LPS. Clinically, AE of IPF is provoked by normal therapeutic interventions. Therefore, we hypothesized that small amounts of LPS may provoke AE of IPF. It has been reported that introducing heat-killed *Propionibacterium acnes*, followed by a subclinical dose challenge of LPS, induces acute and massive liver injury, mimicking fulminant hepatitis.[19] Therefore, in the BLM-induced fibrotic lung, we hypothesized that inflammation induced by small amounts of LPS would cause an excessive inflammatory reaction in the lung, thus, resulting in the induction of AE of IPF.

In animal tissues, nitric oxide (NO) is generated by synthases (NOS).[20] There are three isoforms of NOS: NOS1 - the neuronal form, NOS2 - inducible nitric oxide synthase, and NOS3 - constitutive enzyme primarily found in the endothelium.[21] NO formed by NOS2 in macrophages, neutrophil, and other cells plays multiple roles in the inflammatory response.[20] There have been many reports of excessive NO production, possibly aggravating the pathophysiology of ALI.[22–25] Hence, we hypothesized that NO production could aggravate the pathophysiology of AE of IPF. Moreover, we considered that the small amount of LPS could cause AE of IPF in BLM pretreated rats.

---

*To whom correspondence should be addressed.
E-mail: takemura@med.osaka-cu.ac.jp

doi: 10.3164/jcbn.21-7
©2022 JCBN

J. Clin. Biochem. Nutr. | **March 2022** | vol. 70 | no. 2 | **129–139**

Materials and Methods

Animals. Male Wistar rats (6 weeks old) were purchased from SLC Inc. (Shizuoka, Japan) and were maintained for 1 week before experimental use. All rats were treated according to the specifications outlined in the Guiding Principles for the Care and Use of Laboratory Animals, and the study was approved by the authorities of the local committee on experimental animal research of Osaka City University Medical School (No. 13026).

The rats were randomly segregated into six groups: the BLM (−)/LPS (0) (saline + saline) ($n = 17$), BLM (−)/LPS (0.05) (saline + LPS 0.05 mg/kg) ($n = 23$), BLM (−)/LPS (0.15) (saline + LPS 0.15 mg/kg) ($n = 23$), BLM (+)/LPS (0) (BLM 3 mg/kg + saline) ($n = 23$), BLM (+)/LPS (0.05) (BLM 3 mg/kg + LPS 0.05 mg/kg) ($n = 24$), and BLM (+)/LPS (0.15) (BLM 3 mg/kg + LPS 0.15 mg/kg) ($n = 22$) groups. Rats were anesthetized with sevoflurane delivered into a box, and BLM (3 mg/kg) or saline was intratracheally administered using the oropharyngeal aspiration technique described previously by De Vooght *et al.*[26] Specifically, rats were fixed on a styrofoam board with a plastic bottle and a rubber band; the tongue was extended using forceps, and the liquid was injected into the distal part of the oropharyngeal area, while the nose was closed with fingers. LPS (0.05 or 0.15 mg/kg) or saline was intratracheally administered for 7 days after BLM or saline administration in the same manner. Each tracheal administration volume was 500 μl.

The rats were sacrificed at 24 h, 7 days, or 14 days after LPS administration under three types of mixed anesthetic agents [medetomidine (0.15 mg/0.15 ml/kg), midazolam (2 mg/0.4 ml/kg), butorphanol (2.5 mg/0.5 ml/kg), and saline (1.45 ml/kg)]. For computed tomography (CT) imaging of the lungs, the rats were scanned using Latheta LCT-200 (Hitachi Ltd., Tokyo, Japan). Aortic blood samples were collected using a heparinized syringe from the abdominal aorta, and blood gas analyses were performed using an i-STAT handheld point of the care analyzer (Abbott Point of Care Inc., Princeton, NJ). After perfusion of the abdominal aorta with ice-cold saline, bronchoalveolar lavage (BAL) was performed three times by applying the tracheal cannula to the left lung with 3 ml of saline and the right main bronchus clamped. Later, the BAL fluid (BALF) was centrifuged at 2,500 rpm for 5 min, and the supernatant was stored at −80°C. After the left main and right lower bronchi were ligated, the right lower lung was harvested and was immediately frozen in liquid nitrogen and stored at −80°C. The collected blood was centrifuged at $10,000 \times g$ for 5 min, and the separated plasma was stored at −80°C. The right upper lung was inflated with 2 ml of 10% neutral-buffered formalin via the tracheal cannula. The trachea was clamped, and the right upper lung was harvested and fixed in fresh 10% formalin for 48 h. Tissues were sectioned in the sagittal plane and were embedded in paraffin.

Histochemistry. Sections of the embedded-paraffin samples (4 μm thick) were cut and subjected to hematoxylin-eosin (HE) or Sirius Red (SR) staining, or some other immunohistochemistry procedure. Cell densities stained by SR were quantified using the Olympus cellSens imaging program (ver. 1.7; Olympus Lifescience, Tokyo, Japan). Using a 40× objective, cells stained by SR were measured in three randomly chosen fields. Cell density was expressed as the percentage of cells by stained SR per total cells.

For immunohistochemical analysis of pulmonary alveolar macrophages, the sections were also treated with anti-CD68 antibody (ED-1) (ab31630; Abcam, Cambridge, UK) or anti-inducible NOS2 (BD Transduction Laboratories™, Franklin Lakes, NJ). These histological analyses were performed according to the instructions from the Vectastain ABC-AP kit (Vectastain Laboratories, Burlingame, CA).

Biochemical analysis of plasma and BALF. The pulmonary surfactant protein D (SP-D) and tumor necrosis factor (TNF-α) levels were measured using an SP-D ELISA Kit (YAMASA Corp., Chiba, Japan) and a Rat TNF-α Quantikine ELISA Kit (R&D Systems, Minneapolis, MN) in the plasma and in the BALF, respectively, according to the manufacturers' protocols. The nitrite/nitrate (NOx) levels in the plasma were measured using a NO_2/NO_3 Assay Kit-C II (Colorimetric) (Griess Reagent Kit; Dojindo Laboratories, Kumamoto, Japan). Briefly, plasma was deproteinized with methanol and centrifuged at $12,000 \times g$ for 10 min at 4°C. The supernatant was examined using the assay kit according to the manufacturer's instructions.

Western blot analysis. The right lower lung was homogenized in a sample buffer (50 mM Tris-HCl, pH: 6.8, 2% sodium dodecyl sulfate, 10 mM dithiothreitol, 10% glycerol, and 1 mM phenylmethylsulfonyl fluoride). Lysates were centrifuged at 14,000 rpm for 30 min at 4°C. Proteins (5 μg) from soluble fractions were separated using 10% SDS-polyacrylamide gel electrophoresis and were electroblotted onto polyvinylidene difluoride membranes. Then, the membranes were blocked with 4% blocking ace (No. UKB 40, KAC Co. Ltd, Kyoto, Japan) followed by incubation with NOS2 mouse monoclonal antibody (1:2,000; BD Transduction Laboratories™) at 4°C overnight. Then, the membranes were washed in Tris-buffered saline with 0.5% Tween-20 and were incubated with secondary anti-mouse IgGs (1:20,000; Dako Cytomation, Kyoto, Japan) at room temperature for 1 h followed by incubation with an enhanced chemiluminescence reagent (Amersham, Bucks, UK) for 2 min. Digital images were produced using a luminous image analyzer (LAS-3000 imaging system; Fujifilm, Tokyo, Japan). Densitometric analysis of the protein bands was performed using ImageJ software, ver. 1.47 (National Institutes of Health, Bethesda, MD).

In the ED-1 level measurement, the amount of protein applied was 2 μg. The ED-1 mouse monoclonal antibody (1:4,000; ab31630; Abcam) was used. Similarly, in the nitrotyrosine level measurement, the amount of protein applied was 30 μg. The nitrotyrosine mouse monoclonal antibody (1:2,000; ADI-905-763-100; Enzo Life Sciences, New York, NY) was used.

Quantitative real-time polymerase chain reaction of NOS2 in the lung. Total RNA was extracted from the lungs using a NucleoSpin RNA kit (Takara Bio Inc., Shiga, Japan) and quantified by a NanoDrop 1000 spectrophotometer (Thermo Fisher Scientific, Waltham, MA). Complementary DNA was synthesized using 2 μg of total RNA and a ReverTra Ace qPCR kit (Toyobo, Osaka, Japan). The reaction was performed for 15 min at 37°C, followed by reverse transcriptase inactivation for 5 min at 98°C. Primer/probes for NOS2 (Rn00561646_m1) were purchased from Applied Biosystems (Foster City, CA). Reactions were performed using the commercially available Thunderbird Probe qPCR Mix (QPS-101; Toyobo). mRNA was analyzed with the 7500 Fast Real-time PCR system using TaqMan gene expression assays. Each sample was measured in triplicates and glyceraldehyde 3-phosphate dehydrogenase served as an endogenous control. The cycling conditions were as follows: 95°C for 20 s, followed by 40 cycles of 95°C for 3 s and 60°C for 30 s. The results were analyzed using the comparative cycle threshold ($\Delta\Delta$Ct) method.

Statistical analysis. All values are presented as means ± SDs. Statistical analysis was performed using analysis of variance, and JMP 12 software package (SAS Institute Inc., Cary, NC) was used for all statistical analysis. The correlation coefficient between the NOx and the oxygen partial pressure (pO_2) levels was measured by Pearson's correlation analysis. A value of $p < 0.05$ was considered statistically significant.

Results

Survival rate after LPS administration. In the preliminary study, the survival rate was 30% and 92% in the BLM (+)/LPS
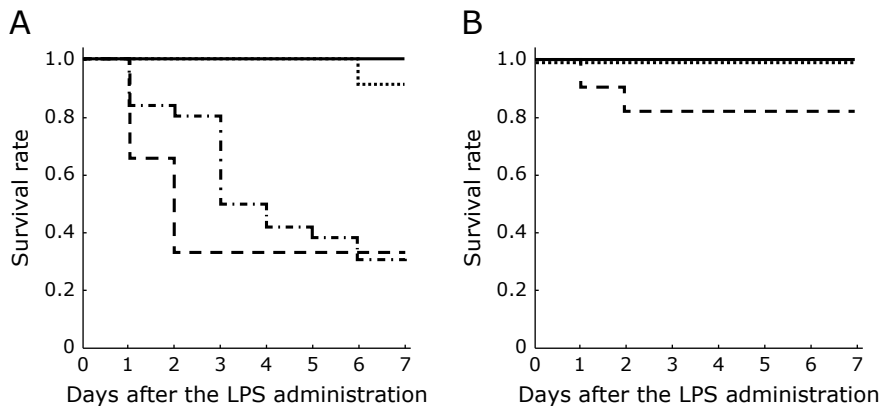
Fig. 1. The survival rate after LPS administration with BLM pretreatment. (A) BLM (3 mg/kg) was intratracheally administered at 7 days before LPS administration [0.1 mg/kg (⋯⋯, *n* = 26), 0.3 mg/kg (– –, *n* = 18), or 0.5 mg/kg (– · –, *n* = 26)] or saline (——, *n* = 32) administration. (B) BLM (3 mg/kg) was intratracheally administered at 7 days before LPS administration [0.05 mg/kg (⋯⋯, *n* = 12) or 0.15 mg/kg (– –, *n* = 12)] or saline (——, *n* = 32) administration. BLM, bleomycin; LPS, lipopolysaccharide.
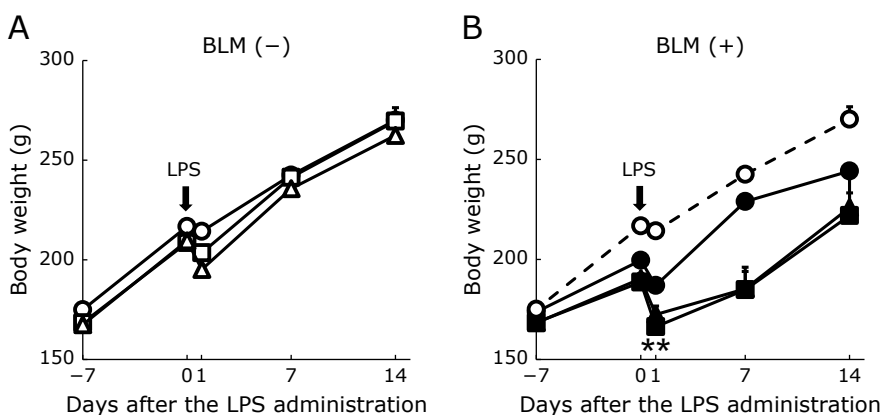
Fig. 2. Changes in the body weights of rats after BLM administration. BLM (3 mg/kg) or saline was intratracheally administered at 7 days before LPS (0.05 or 0.15 mg/kg) or saline administration. (A) Rats were segregated into three groups: ○: BLM (–)/LPS (0); □: BLM (–)/LPS (0.05); and △: BLM (–)/LPS (0.15). (B) Rats were segregated into four groups: ●: BLM (+)/LPS (0); ■: BLM (+)/LPS (0.05); ▲: BLM (+)/LPS (0.15); and ○: BLM (–)/LPS (0). Values are presented as means ± SDs (*n* = 22–24). **p<0.01 vs BLM (–)/LPS (0). BLM, bleomycin; LPS, lipopolysaccharide.

(>0.3 mg/kg) and BLM (+)/LPS (0.1 mg/kg) groups, respectively (Fig. 1A). The survival rate was significantly lower in the BLM (+)/LPS (>0.3 mg/kg) than in the BLM (+)/LPS (0) group (*p*<0.01). Therefore, the analyzable LPS doses were determined as 0.05 and 0.15 mg/kg, around the dose of 0.1 mg/kg.

The survival rates were 100% and 83% in the BLM (+)/LPS (0.05) and BLM (+)/LPS (0.15) groups (Fig. 1B), respectively. Moreover, the survival rate was 100% in the BLM (–)/LPS (0.05 or 0.15) group.

Changes in the body weight. In the BLM-free groups, the body weight increased in a time-dependent manner (Fig. 2A). The weight of rats in the BLM (–)/LPS (0.05 or 0.15) groups transiently decreased after LPS administration but increased in the BLM (–)/LPS (0) group (Fig. 2A). In contrast, the weight of rats in the BLM (+)/LPS (0.05 or 0.15) group decreased after LPS administration and decreased for 7 days (Fig. 2B). Besides, in the BLM (+)/LPS (0) group, the body weight of the rats at 24 h after LPS administration was lower than that of the BLM (–)/LPS (0) group (*p*<0.01) (Fig. 2B). Furthermore, in the BLM (+)/LPS (0.05 or 0.15) group, the body weight of rats at 24 h after LPS administration was lower than that in the BLM (–)/LPS (0.05 or 0.15) group.

CT images of the rat lungs. CT images of the lungs at 24 h after LPS administration are shown in Fig. 3. The lung images in the BLM (+)/LPS (0) and BLM (–)/LPS (0.05 or 0.15) groups showed little infiltrative shadows. The lung images in the BLM (+)/LPS (0.05 or 0.15) group showed more visible infiltrative shadows than those in the BLM (–)/LPS (0) group, which were similar to ARDS.

Histological findings of the rat lungs. Lung tissues subjected to HE and SR staining showed normal structure in the BLM (–)/LPS (0) group (Fig. 4A). In the BLM (+)/LPS (0, 0.05, or 0.15) group, lung histology showed significant progression of fibrosis (Fig. 4D–F). In the BLM (–)/LPS (0.05 or 0.15) group, lung histology showed infiltration of inflammatory cells (Fig. 4B and C). In the BLM (+)/LPS (0.05 or 0.15) group, prominent infiltration of inflammatory cells and alveolar enlargement were observed (Fig. 4E and F). In the BLM (+)/LPS (0, 0.05, or 0.15) groups, cells stained by SR (34.0 ± 3.7%, 41.5 ± 1.1%, or 43.1 ± 0.7%, respectively) were wider than those in the BLM (–)/LPS (0, 0.05, or 0.15) groups (11.2 ± 2.4%, 8.0 ± 1.0%, or 7.3 ± 1.3%, respectively) (*p*<0.01) (Fig. 5).

Arterial blood gas analysis. In the BLM (–)/LPS (0, 0.05, or 0.15) group, the arterial blood gas levels at 24 h after LPS administration were within the normal ranges. In contrast, in the BLM (+)/LPS (0, 0.05, or 0.15) group, the pO₂ levels were significantly low (81.0 ± 3.4, 64.0 ± 6.2, or 61.0 ± 8.3 mmHg, respectively) (*p*<0.01) (Fig. 6A-1), the carbon dioxide partial
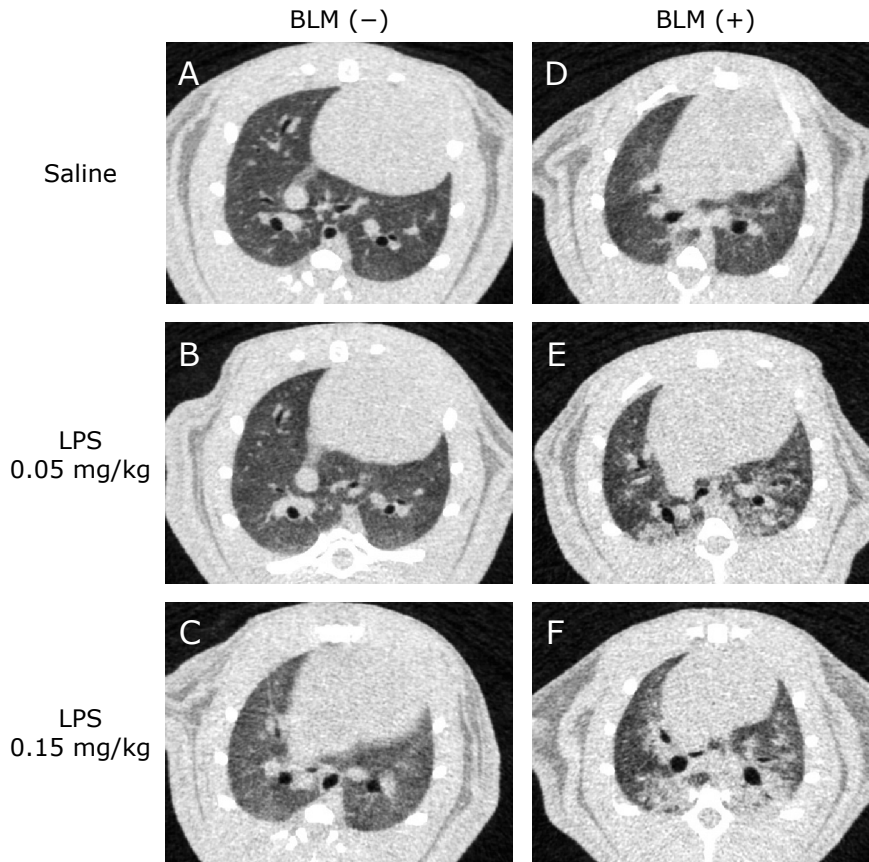
Fig. 3. CT images of rat lungs at 24 h after LPS administration (0.05 or 0.15 mg/kg). Rats were treated as described in Fig. 2. (A) BLM (–)/LPS (0); (B) BLM (–)/LPS (0.05); (C) BLM (–)/LPS (0.15); (D) BLM (+)/LPS (0); (E) BLM (+)/LPS (0.05); and (F) BLM (+)/LPS (0.15). BLM, bleomycin; LPS, lipopolysaccharide; CT, computed tomography.
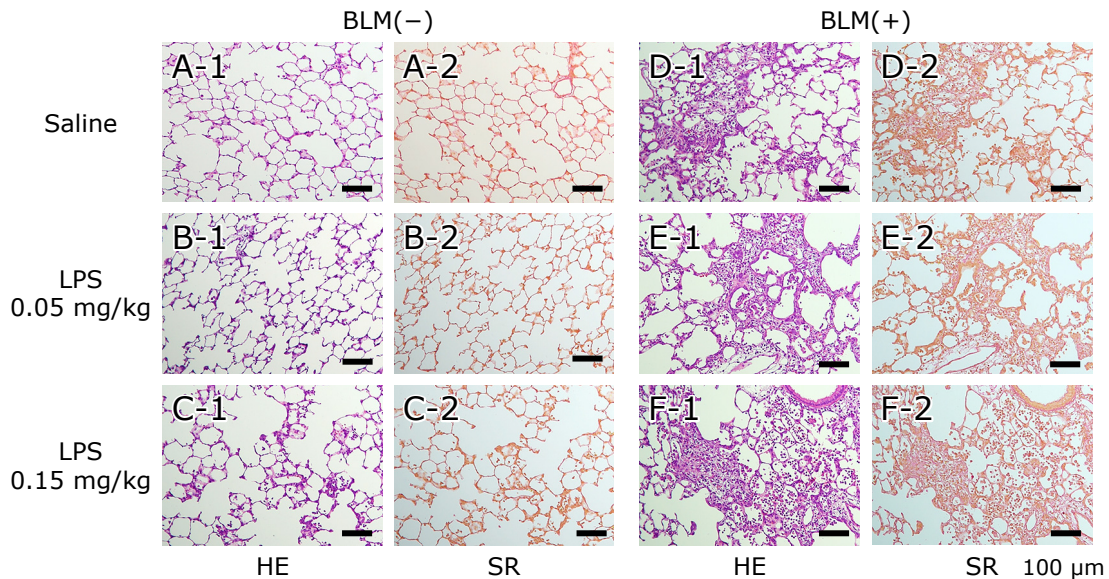

Fig. 4. Histological findings of rat lungs stained with HE or SR staining at 24 h after LPS administration (0.05 or 0.15 mg/kg). Rats were treated as described in Fig. 2. (A) BLM (–)/LPS (0); (B) BLM (–)/LPS (0.05); (C) BLM (–)/LPS (0.15); (D) BLM (+)/LPS (0); (E) BLM (+)/LPS (0.05); and (F) BLM (+)/LPS (0.15). HE, hematoxylin-eosin; SR, Sirius Red; BLM, bleomycin; LPS, lipopolysaccharide. See color figure in the on-line version.
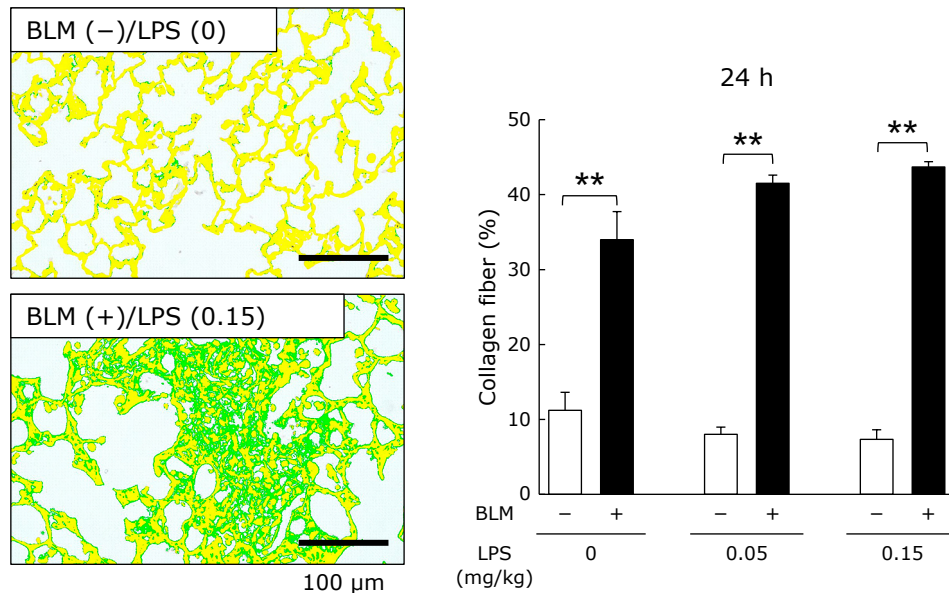
Fig. 5. Collagen fiber in the lung. Rats were treated as described in Fig. 2. The green field represents cells stained by SR, and the yellow field represents those not stained by SR. Values are presented as means ± SDs (*n* = 3). **p<0.01 vs BLM (–)/LPS (each dose). Bar graph shows BLM (–) (open columns) and BLM (+) (shaded columns). LPS, lipopolysaccharide; BLM, bleomycin. HE, hematoxylin-eosin; SR, Sirius Red; BLM, bleomycin; LPS, lipopolysaccharide. See color figure in the on-line version.

pressure (pCO$_2$) was significantly high (51.2 ± 5.9, 60.6 ± 4.3 or 62.5 ± 4.0 mmHg, respectively) (*p*<0.01) (Fig. 6B-1), and the pH was significantly low (7.3 ± 0.05, 7.3 ± 0.03 or 7.3 ± 0.02, respectively) (*p*<0.01) (Fig. 6C-1) at 24 h after LPS administration. The pO$_2$ levels significantly decreased in the BLM (+)/LPS (0.05 or 0.15) groups than in the BLM (+)/LPS (0) group (*p*<0.01) (Fig. 6A-1). However, at 14 days after LPS administration, pO$_2$, pCO$_2$, and pH were normalized, indicating recovery of respiratory failure (Fig. 6A-2, A-3, B-2, B-3, C-2, and C-3). One of the clinical definitions of AE of IPF is a decrease in pO$_2$ by >10 mmHg. The pO$_2$ levels were significantly lower in the BLM (+)/LPS (0.05 or 0.15) than in the BLM (+)/LPS (0) group by >10 mmHg (*p* = 0.04 or *p* = 0.02).

Levels of plasma SP-D. In the BLM (+)/LPS (0, 0.05, or 0.15) group, the levels of plasma SP-D were high at 24 h after LPS administration (521.3 ± 52.6, 574.7 ± 40.2, or 546.0 ± 43.9 ng/ml, respectively) than those in the BLM (−)/LPS (0, 0.05, or 0.15) group (137.8 ± 6.7, 204.3 ± 9.8, or 221.0 ± 15.4 ng/ml, respectively) (*p*<0.01) (Fig. 7A). In the BLM (−)/LPS (0, 0.05, or 0.15 mg/kg) group, the levels of plasma SP-D did not change at any time point (Fig. 7B) (BLM (−)/LPS (0.05 or 0.15) vs BLM (−)/LPS (0): at 24 h after LPS administration; *p* = 0.15 and *p* = 0.08, respectively; at 7 days; *p* = 0.5 and *p* = 0.65, respectively; at 14 days, *p* = 0.62 and *p* = 0.50, respectively). Furthermore, the plasma SP-D levels significantly increased at all time points in the BLM (+)/LPS (0, 0.05, or 0.15) than in the BLM (−)/LPS (0) group (*p*<0.01) (Fig. 7C). The plasma SP-D levels peaked at 7 days after LPS administration (Fig. 7C).

Levels of NOx in plasma. In the BLM (−)/LPS (0, 0.05, or 0.15) group, the levels of NOx in plasma at 24 h after LPS administration were within the normal ranges (44.9 ± 5.2, 63.1 ± 2.6, or 52.9 ± 6.3 µM, respectively) (BLM (−)/LPS (0.05 or 0.15) vs BLM (−)/LPS (0): *p* = 0.06 and *p* = 0.38, respectively) (Fig. 8A). The levels of NOx were significantly higher in the BLM (+)/LPS (0.05 or 0.15) (85.1 ± 7.2 or 94.5 ± 9.4, respectively) than in the BLM (+)/LPS (0) (52.4 ± 5.3) and BLM (−)/LPS (0.05 or 0.15) groups (63.0 ± 2.6 or 52.9 ± 6.3) (*p*<0.01) (Fig. 8A). However, at 7 days after LPS administration, the NOx levels were normalized in all groups (Fig. 8B and C). In addition,

in the BLM (−) groups, there was no correlation between the NOx and pO$_2$ levels in the plasma at 24 h after (Fig. 9A); however, there was a strong correlation between these two variables in the BLM (+) groups (*r* = 0.76, *p*<0.01) (Fig. 10B).

Levels of NOS2 proteins and mRNA in the lungs. In the BLM (−)/LPS (0, 0.05 or 0.15) and BLM (+)/LPS (0) groups, the NOS2 levels in the lung showed no changes at 24 h after LPS administration by Western blot analysis (0.002 ± 0.002, 0.2 ± 0.04, or 0.9 ± 0.2 and 0.02 ± 0.02, respectively) (*p* = 0.66, *p* = 0.06, or *p* = 0.97; In the BLM (−)/LPS (0.05 or 0.15 mg/kg) and BLM (+)/LPS (0 mg/kg) vs In the BLM (−)/LPS (0)) (Fig. 10A). In the BLM (+)/LPS (0.05 or 0.15) group, the NOS2 levels in the lung at 24 h after LPS administration (1.0 ± 0.2 or 2.2 ± 0.7, respectively) were significantly higher than those in the BLM (−)/LPS (0.05 or 0.15) group (0.2 ± 0.04 or 0.9 ± 0.2, respectively) (*p*<0.01) (Fig. 10A). However, the NOS2 levels dropped to 0 at 7 days after LPS administration (Fig. 10B and C). The NOS2 mRNA expressions in the lung at 24 h after LPS administration were significantly higher in the BLM (+)/LPS (0.05 or 0.15) (21.4 ± 0.08 or 34.0 ± 0.4, respectively) than in the BLM (+)/LPS (0) (1.62 ± 0.2) (*p*<0.01) and the BLM (−)/LPS (0.05 or 0.15) group (11.0 ± 0.3 or 19.0 ± 0.3, respectively) (Fig. 11).

Infiltration of macrophage and NOS2 in the lung. ED-1 (stained in the macrophages) was highly stained in the BLM (+)/LPS (0.05 or 0.15) groups (Fig. 12E-1 and F-1). Furthermore, NOS2 positive cells were colocalized with ED1 positive cells (Fig. 12E-2 and F-2).

In addition, in the BLM (−)/LPS (0.05 or 0.15) groups, the ED-1 levels in the lung were significantly higher than those in the BLM (−)/LPS (0) group (*p*<0.05) (Fig. 13). However, in the BLM (+)/LPS (0.05 or 0.15) groups, the ED-1 levels in the lung were higher than those in the BLM (−)/LPS (0.05 or 0.15) groups (BLM (+)/LPS (0.05) vs BLM (−)/LPS (0.05), *p*<0.05; BLM (+)/LPS (0.15) vs BLM (−)/LPS (0.15), *p* = 0.05) (Fig. 13).

Levels of nitrotyrosine in the lung. In the BLM (−)/LPS (0, 0.05, or 0.15) group, the levels of nitrotyrosine in the lung did not appear (Fig. 14). However, in the BLM (+) groups, the levels of nitrotyrosine increased in a LPS dose-dependent manner.
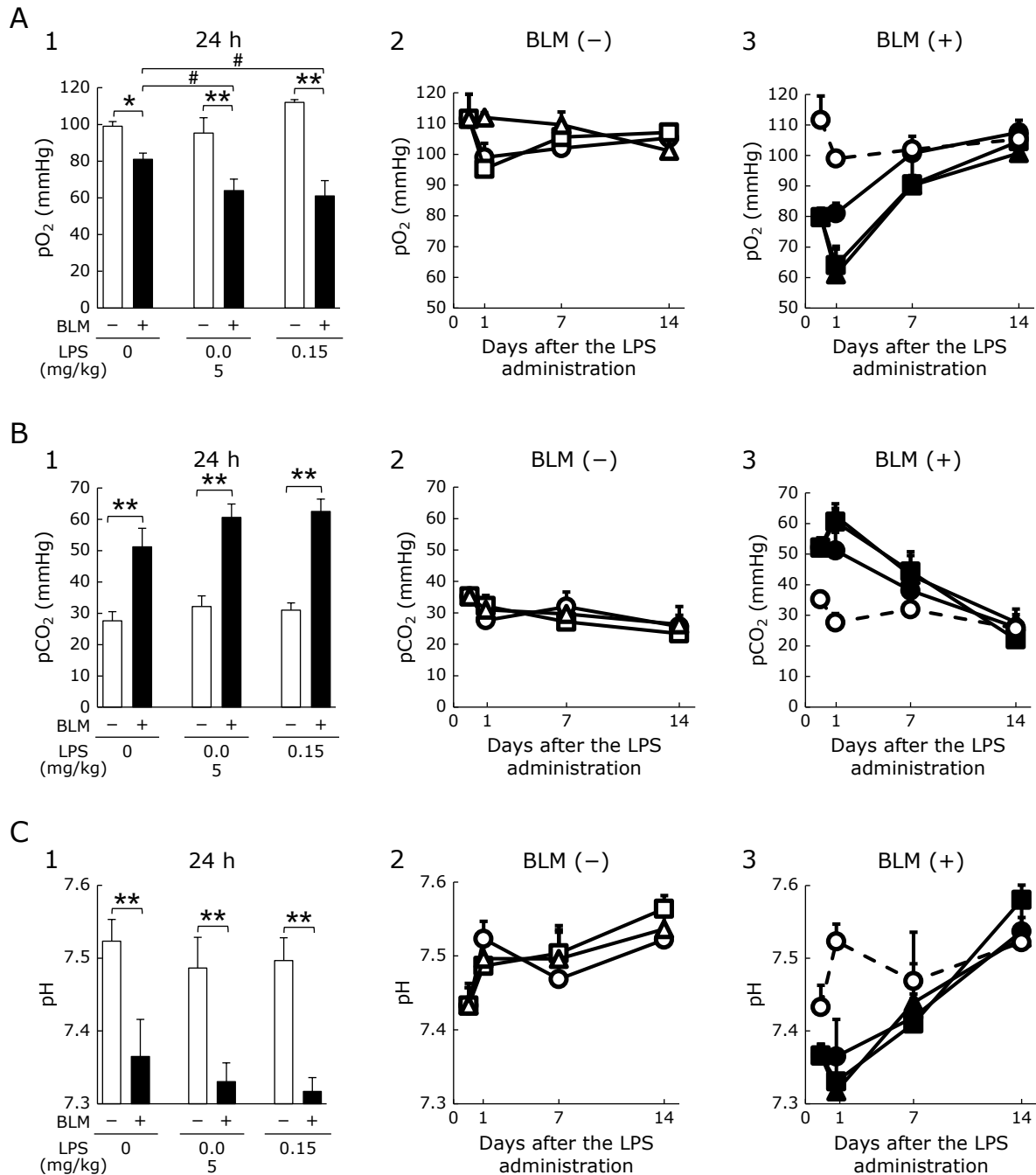
Fig. 6. Arterial blood gas analyses. Rats were treated as described in Fig. 2. 1: Bar graphs show each parameter at 24 h after LPS treatment (0.05 or 0.15 mg/kg). Values are presented as means ± SDs ($n = 3$–6). *$p<0.05$, **$p<0.01$ vs BLM (–)/LPS (each dose), #$p<0.05$ vs BLM (+)/LPS (0). Open and shaded columns correspond to BLM (–) and BLM (+), respectively. (A) oxygen partial pressure (pO_2); (B) carbon dioxide partial pressure (pCO_2); and (C) pH. 2 and 3: Time course of 14 days after LPS treatment. ○: BLM (–)/LPS (0); □: BLM (–)/LPS (0.05); △: BLM (–)/LPS (0.15); ●: BLM (+)/LPS (0); ■: BLM (+)/LPS (0.05); and ▲: BLM (+)/LPS (0.15). LPS, lipopolysaccharide; BLM, bleomycin.

Levels of TNF-α in BALF. In the BLM (−)/LPS (0) and BLM (+)/LPS (0) groups, the TNF-α level in the BALF was 0. In the BLM (−)/LPS (0.05 or 0.15) groups, the TNF-α levels in the BALF did not increase (2.0 ± 1.3 or 0.13 ± 0.1 pg/ml, respectively) (Fig. 15). However, in the BLM (+)/LPS (0.05 or 0.15) group, the levels of TNF-α in the BALF increased (22.3 ± 4.3 or 19.2 ± 5.0 pg/ml, respectively) (Fig. 15).

Discussion

This study indicated that inflammation induced by a small amount of LPS (0.05 or 0.15 mg/kg) could cause an excessive inflammatory reaction with NO elevation in BLM-induced pulmonary fibrosis in rats, and this model could be used to mimic AE of IPF.

AE of IPF is clinically defined as a progressing symptom of dyspnea, honeycomb lung findings, new ground-glass opacity and/or infiltrative shadows on CT, and a decrease in the pO_2
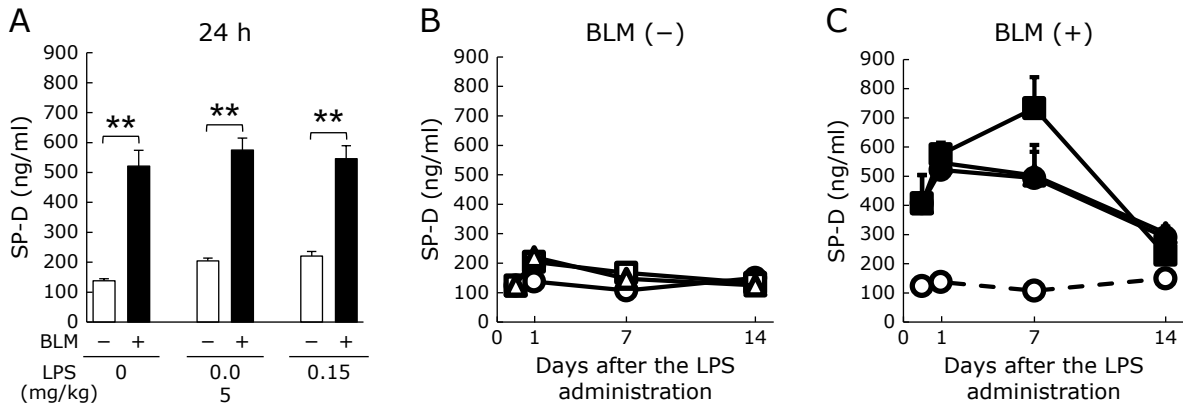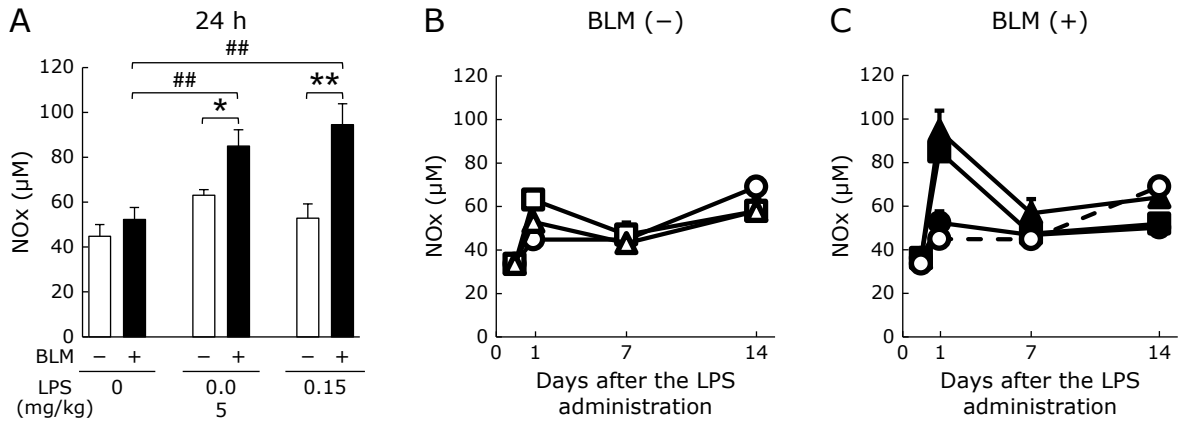
Fig. 7. The pulmonary SP-D levels in the plasma. Rats were treated as described in Fig. 2. SP-D levels in the plasma were measured using the enzyme-linked immunosorbent assay. (A) bar graph shows the plasma levels of SP-D at 24 h after LPS administration (0.05 or 0.15 mg/kg). Values are presented as means ± SDs (n = 11–13). **$p<0.01$ vs BLM (–)/LPS (each dose). Open and shaded columns correspond to BLM (–) and BLM (+), respectively. (B, C) time course of the plasma SP-D levels. ○: BLM (–)/LPS (0); □: BLM (–)/LPS (0.05); △: BLM (–)/LPS (0.15); ●: BLM (+)/LPS (0); ■: BLM (+)/LPS (0.05); and ▲: BLM (+)/LPS (0.15). LPS, lipopolysaccharide; BLM, bleomycin; SP-D, surfactant protein D.

Fig. 8. The NOx levels in the plasma. Rats were treated as described in Fig. 2. The NOx levels in the plasma were measured using the enzyme linked immunosorbent assay. (A) The NOx levels in the plasma at 24 h after LPS administration (0.05 or 0.15 mg/kg) are presented. Values are presented as means ± SDs (n = 3–12). *$p<0.05$, **$p<0.01$ vs BLM (–)/LPS (each dose), ##$p<0.01$ vs BLM (+)/LPS (0). Open and shaded columns correspond to BLM (–) and BLM (+), respectively. (B, C) Time course changes of the NOx levels in the plasma. ○: BLM (–)/LPS (0); □: BLM (–)/LPS (0.05); △: BLM (–)/LPS (0.15); ●: BLM (+)/LPS (0); ■: BLM (+)/LPS (0.05); and ▲: BLM (+)/LPS (0.15). LPS, lipopolysaccharide; BLM, bleomycin; NOx, nitrite + nitrate.
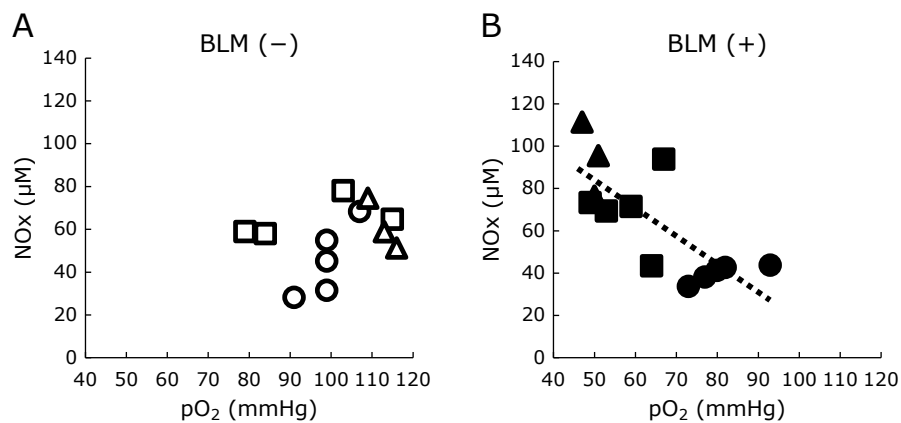

Fig. 9. The correlation of the NOx and pO₂ levels in the plasma. Rats were treated as described in Fig. 2. ○: BLM (–)/LPS (0); □: BLM (–)/LPS (0.05); △: BLM (–)/LPS (0.15); ●: BLM (+)/LPS (0); ■: BLM (+)/LPS (0.05); and ▲: BLM (+)/LPS (0.15). LPS, lipopolysaccharide; BLM, bleomycin; NOx, nitrite + nitrate.
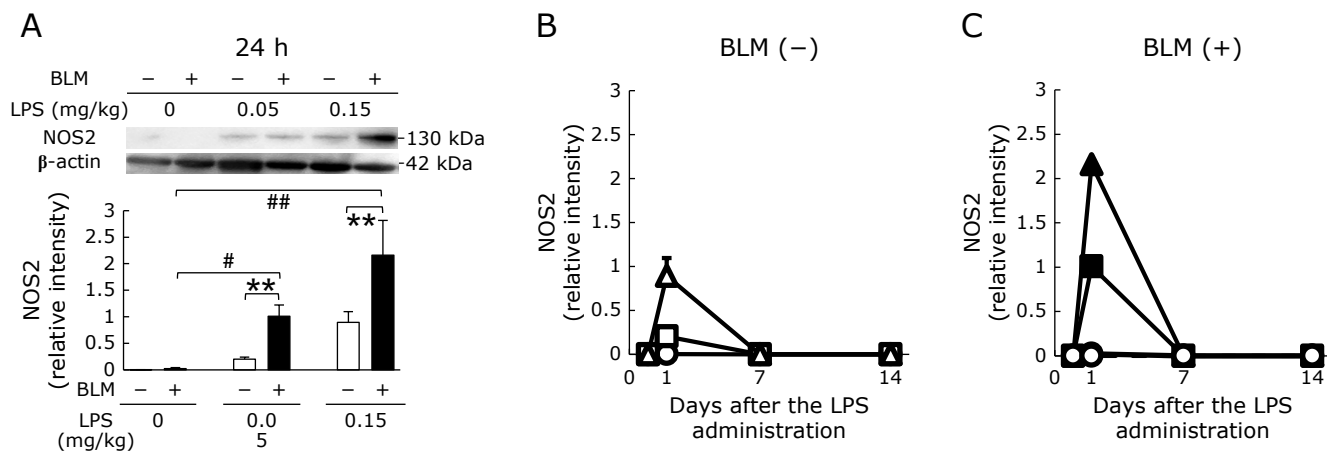
Fig. 10. The anti-inducible NOS2 levels in the lungs. Rats were treated as described in Fig. 2. NOS2 levels in the lungs were measured using Western blotting. (A) The NOS2 levels in the lungs at 24 h after LPS administration (0.05 or 0.15 mg/kg). Values are presented as means ± SDs (n = 3–12). **$p<0.01$ vs BLM (–)/LPS (each dose), #$p<0.05$, ##$p<0.01$ vs BLM (+)/LPS (0). Open columns are BLM (–) and shaded columns are BLM (+). (B, C) Time course of the NOS2 levels in the lungs. ○: BLM (–)/LPS (0); □: BLM (–)/LPS (0.05); △: BLM (–)/LPS (0.15); ●: BLM (+)/LPS (0); ■: BLM (+)/LPS (0.05); and ▲: BLM (+)/LPS (0.15). LPS, lipopolysaccharide; BLM, bleomycin; NOS2, nitric oxide synthase.
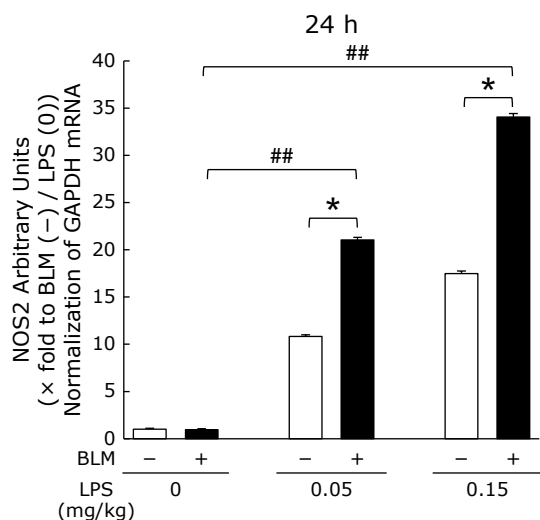

Fig. 11. The NOS2 mRNA expression in the lungs. Rats were treated as described in Fig. 2. The NOS2 mRNA levels in the lungs were measured by quantitative reverse transcriptase-PCR. The NOS2 mRNA levels in the lungs at 24 h after LPS administration (0.05 or 0.15 mg/kg) are presented. Values are presented as means ± SDs (n = 3–12). *$p<0.05$ vs BLM (–)/LPS (each dose), ##$p<0.01$ vs BLM (+)/LPS (0). The open and closed columns correspond to BLM (–) and BLM (+), respectively. LPS, lipopolysaccharide; BLM, bleomycin; NOS2, nitric oxide synthase.

levels by >10 mmHg. The reference findings included increased the C-reactive protein, lactate dehydrogenase, Krebs von den Lungen-6, and SP-D levels in the blood.[2] Therapeutic interventions, especially surgical treatments, have been reported to provoke AE of IPF.[3] According to the clinical definition, our study demonstrated that a small amount of LPS (0.05 or 0.15 mg/kg) administration after BLM-induced pulmonary fibrosis could induce dyspnea (Fig. 6), increase consumption, and decrease body weight because of increased exhaustion of physical strength. Furthermore, the CT images of the lungs showed more infiltrative shadows (Fig. 3). In addition to the results of low pO_2 levels in the arterial blood (Fig. 6A), and the high levels of TNFα in the BALF (Fig. 13), our study reinforced

the definition of AE of IPF. The LPS doses were approximately one-tenth of those of the experimental models of pneumonia or ALI.[11,18] Therefore, this model could mimic AE of IPF clinically provoked by therapeutic interventions or minor infections.

A mouse model combining the two types of injuries has been reported.[17] In this report, the LPS dose was 0.5 mg/kg, which is approximately the same as that used in ALI/ARDS animal models.[11,18] This reaction may have been normal severe pneumonia. Our model could better mimic AE of IPF clinically provoked by therapeutic interventions or minor infections. One of the commonly used animal models of fulminant hepatitis is mice injected with heat-killed P. acnes, followed by small amounts of LPS.[27,28] In this model of fulminant hepatitis, liver injury is pathophysiologically classified into two phases: the priming phase induced by Propionibacterium acnes and the eliciting phase, in which LPS activates the granuloma-forming cells, leading to severe liver injury.[27,29–31] Similarly, the model of AE of IPF in our study has two phases: the priming phase, in which the administration of BLM induces pulmonary fibrosis, and the eliciting phase, in which LPS induces inflammation and leads to dyspnea and ALI. The AE response was similar to fulminant hepatitis response.

Generally, the pathophysiology of AE of IPF is unknown, but our study suggested that AE was associated with increased NO levels. Recently, there have been many reports that NO likely aggravates the pathophysiology of ALI.[22–25] In addition, it has been reported that the pulmonary expressions of NOS2 and NO production were enhanced in animal models and humans with ALI.[32–37] In one of these studies, it was reported that the total NOx levels in patients with ALI/ARDS (83 ± 14 μM) were significantly higher than those in normal volunteers (26 ± 2.7 μM).[37] In addition, the large amounts of LPS are known to markedly induce the expression of NOS2 in the lung tissue, thus, leading to increased NO production.[38–40] Given the small amounts of LPS in our study (0.05 or 0.15 mg/kg), the levels of NOS2 in the lung and the NOx levels in the plasma slightly increased in the BLM-free group (58 ± 3.6 μM). Nevertheless, LPS administration significantly increased the NOS2 levels in the lung and the NOx levels in the plasma in the BLM-pretreated groups (90 ± 5.9 μM) (Fig. 8). In the immunological staining of lung tissues, NOS2 positive cells were colocalized with ED-1 positive cells, suggesting that pulmonary macrophages expressed NOS2 (Fig. 12). In this study, there was a strong correlation
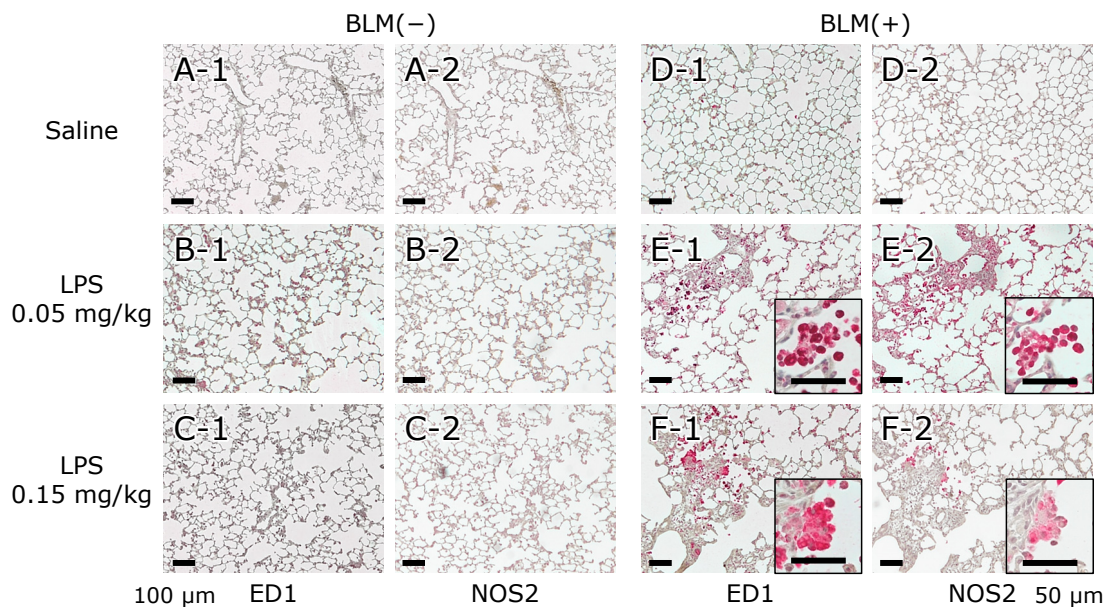
Fig. 12. Histological findings of anti-CD68 antibody (ED-1) or anti-inducible NOS2 expression in the rat lungs. Rats were treated as described in Fig. 2. The lungs were stained with anti-ED1 or anti-NOS2 antibody at 24 h after LPS administration (0.05 or 0.15 mg/kg). (A) BLM (–)/LPS (0); (B) BLM (–)/LPS (0.05); (C) BLM (–)/LPS (0.15); (D) BLM (+)/LPS (0); (E) BLM (+)/LPS (0.05); (F) BLM (+)/LPS (0.15). LPS, lipopolysaccharide; BLM, bleomycin; NOS2, nitric oxide synthase. See color figure in the on-line version.
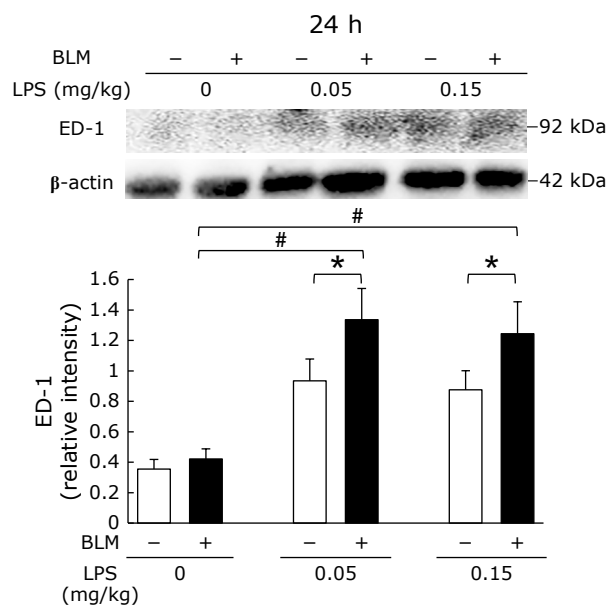

Fig. 13. The ED-1 levels in the lungs. Rats were treated as described in Fig. 2. The ED-1 levels in the lungs were measured using Western blotting. The ED-1 levels in the lungs, measured at 24 h after LPS administration (0.05 or 0.15 mg/kg), are presented. Values are presented as means ± SDs ($n = 3–12$). *$p<0.05$ vs BLM (–)/LPS (each dose), #$p<0.05$ vs BLM (+)/LPS (0). The open and closed columns correspond to BLM (–) and BLM (+), respectively. LPS, lipopolysaccharide; BLM, bleomycin.
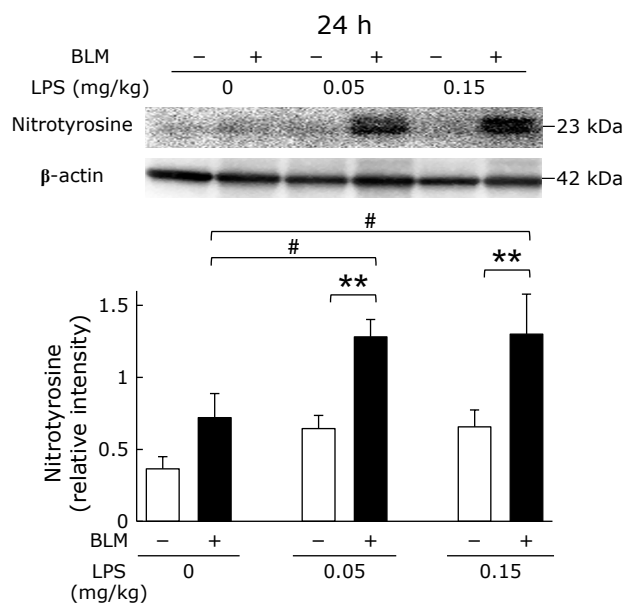

Fig. 14. The nitrotyrosine levels in the lungs. Rats were treated as described in Fig. 2. The nitrotyrosine levels in the lungs were measured using Western blotting. The nitrotyrosine levels in the lungs, measured at 24 h after LPS administration (0.05 or 0.15 mg/kg), are presented. Values are presented as means ± SDs ($n = 3–12$). **$p<0.01$ vs BLM (–)/LPS (each dose), #$p<0.05$ vs BLM (+)/LPS (0). The open and closed columns correspond to BLM (–) and BLM (+), respectively. LPS, lipopolysaccharide; BLM, bleomycin.

between the NOx and pO$_2$ levels in plasma at 24 h after LPS administration in BLM-treated groups (Fig. 9). The excessive NO production may be one of the causes of AE of IPF. In this model, it is considered that NOS2 expression in pulmonary macrophages contributes significantly to increase NO production during lung injury by endotoxin administration.[39,41] In our model, there were many NOS2-positive macrophages (Fig. 12). Therefore, it is expected that selective NOS2 inhibition in pulmonary macrophages may be a beneficial therapeutic strategy for AE of IPF. In addition, as the nitrotyrosine levels in the BLM-treated lung increased in an LPS-dose dependent manner, it is suggested that NO and O$_2^-$ production are concerted in AE.
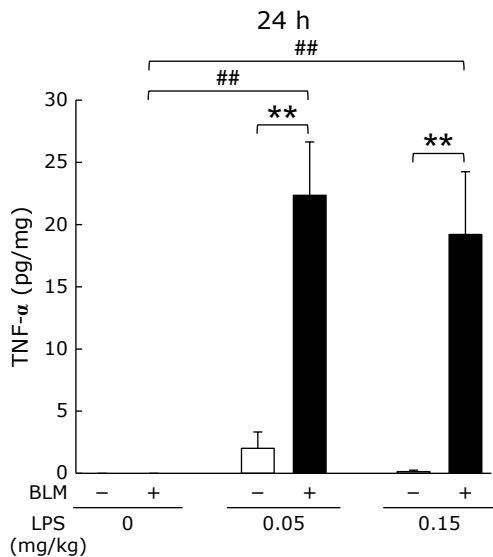
Fig. 15. The TNF-α levels in the BALF at 24 h after LPS administration (0.05 or 0.15 mg/kg). Rats were treated as described in Fig. 2. BALF samples were collected as described in the Methods section. The TNF-α levels in the BALF were measured using the enzyme-linked immuno-sorbent assay. Values are presented as means ± SDs (n = 7–12). $^{\#\#}p<0.01$ vs BLM (+)/LPS (0), $^{**}p<0.01$ vs BLM (–)/LPS (each dose). Bar graph shows BLM (–) (open columns) and BLM (+) (shaded columns). LPS, lipopolysaccharide; BLM, bleomycin; TNF-α, tumor necrosis factor; BALF, bronchoalveolar lavage fluid.

NO is also used in the treatment of respiratory failure. The dose of NO inhalation in the treatment is very low (approximately 5 ppm). In contrast, the production of NO in this study was large (approximately 40–100 μM). The small amount of NO presented a vasodilator action and anti-coagulant activity among others.[42] In contrast, the large amounts of NO induce harmful cytotoxic effects. Thus, it seems that the NO usage is a double-edged sword regarding its biological effects.

Further, it has been reported that recombinant soluble TNFR-beta and Vitamin D3 are effective in cases of pulmonary fibrosis.[43,44] Thus, it is necessary to examine whether it is also effective in this model.

In conclusion, this study showed that inflammation induced by small amounts of LPS in BLM-treated rat mimics the conditions of AE of IPF. In addition, the results suggested that excessive NO production in the lung is an important indicator for AE of IPF. It is expected that selective NOS2 inhibition targeting pulmonary macrophages would be a beneficial therapeutic strategy for AE of IPF.

Author Contributions

Acknowledgments

Abbreviations

AE	acute exacerbation
ALI/ARDS	acute lung injury/acute respiratory distress syndrome
BAL	bronchoalveolar lavage
BALF	BAL fluid
BLM	bleomycin
CRDs	chronic respiratory diseases
CT	computed tomography
ED-1	anti-CD68 antibody
HE	hematoxylin-eosin
IPF	Idiopathic pulmonary fibrosis
LPS	lipopolysaccharide
NO	nitric oxide
NOS	nitric oxide synthase
NOx	nitrite + nitrate
SP-D	pulmonary surfactant protein D
SR	Sirius Red
TNF-α	tumor necrosis factor

Conflict of Interest

No potential conflicts of interest were disclosed.

References

1 Chronic respiratory diseases. https://www.who.int/health-topics/chronic-respiratory-diseases#tab=tab_1. Accessed 8 Jul 2019

2 Kondoh Y, Taniguchi H, Kawabata Y, *et al*. Acute exacerbation in idiopathic pulmonary fibrosis. Analysis of clinical and pathologic findings in three cases. *Chest* 1993; **103**: 1808–1812.

3 Minegishi Y, Takenaka K, Mizutani H, *et al*. Exacerbation of idiopathic interstitial pneumonias associated with lung cancer therapy. *Intern Med* 2009; **48**: 665–672.

4 Antoniou KM, Wells AU. Acute exacerbations of idiopathic pulmonary fibrosis. *Respiration* 2013; **86**: 265–274.

5 Chiyo M, Sekine Y, Iwata T, *et al*. Impact of interstitial lung disease on surgical morbidity and mortality for lung cancer: analyses of short-term and long-term outcomes. *J Thorac Cardiovasc Surg* 2003; **126**: 1141–1146.

6 Kumar P, Goldstraw P, Yamada K, *et al*. Pulmonary fibrosis and lung cancer:

risk and benefit analysis of pulmonary resection. *J Thorac Cardiovasc Surg* 2003; **125**: 1321–1327.

7 Koizumi K, Hirata T, Hirai K, *et al*. Surgical treatment of lung cancer combined with interstitial pneumonia: the effect of surgical approach on post-operative acute exacerbation. *Ann Thorac Cardiovasc Surg* 2004; **10**: 340–346.

8 Watanabe A, Kawaharada N, Higami T. Postoperative acute exacerbation of IPF after lung resection for primary lung cancer. *Pulm Med* 2011; **2011**: 960316.

9 Sato T, Teramukai S, Kondo H, *et al*. Impact and predictors of acute exacerbation of interstitial lung diseases after pulmonary resection for lung cancer. *J Thorac Cardiovasc Surg* 2014; **147**: 1604–1611.e1603.

10 Reutershan J, Basit A, Galkina EV, Ley K. Sequential recruitment of neutrophils into lung and bronchoalveolar lavage fluid in LPS-induced acute

lung injury. *Am J Physiol Lung Cell Mol Physiol* 2005; **289**: L807–L815.

11 Rojas M, Woods CR, Mora AL, Xu J, Brigham KL. Endotoxin-induced lung injury in mice: structural, functional, and biochemical responses. *Am J Physiol Lung Cell Mol Physiol* 2005; **288**: L333–L341.

12 de Souza Xavier Costa N, Ribeiro Júnior G, Dos Santos Alemany AA, *et al*. Early and late pulmonary effects of nebulized LPS in mice: An acute lung injury model. *PLoS One* 2017; **12**: e0185474.

13 Mei SH, McCarter SD, Deng Y, Parker CH, Liles WC, Stewart DJ. Prevention of LPS-induced acute lung injury in mice by mesenchymal stem cells overexpressing angiopoietin 1. *PLoS Med* 2007; **4**: e269.

14 Brigham KL, Meyrick B. Endotoxin and lung injury. *Am Rev Respir Dis* 1986; **133**: 913–927.

15 Wang HM, Bodenstein M, Markstaller K. Overview of the pathology of three widely used animal models of acute lung injury. *Eur Surg Res* 2008; **40**: 305–316.

16 Moore BB, Hogaboam CM. Murine models of pulmonary fibrosis. *Am J Physiol Lung Cell Mol Physiol* 2008; **294**: L152–L160.

17 Kimura T, Nojiri T, Hosoda H, *et al*. Exacerbation of bleomycin-induced injury by lipopolysaccharide in mice: establishment of a mouse model for acute exacerbation of interstitial lung diseases. *Eur J Cardiothorac Surg* 2015; **48**: e85–e91.

18 Tsubochi H, Suzuki S, Kubo H, *et al*. Early changes in alveolar fluid clearance by nitric oxide after endotoxin instillation in rats. *Am J Respir Crit Care Med* 2003; **167**: 205–210.

19 Tsuji H, Harada A, Mukaida N, *et al*. Tumor necrosis factor receptor p55 is essential for intrahepatic granuloma formation and hepatocellular apoptosis in a murine model of bacterium-induced fulminant hepatitis. *Infect Immun* 1997; **65**: 1892–1898.

20 Michel T, Feron O. Nitric oxide synthases: which, where, how, and why? *J Clin Invest* 1997; **100**: 2146–2152.

21 Ignarro LJ. Nitric oxide as a unique signaling molecule in the vascular system: a historical overview. *J Physiol Pharmacol* 2002; **53 (4 Pt 1)**: 503–514.

22 Mehta S. The effects of nitric oxide in acute lung injury. *Vascul Pharmacol* 2005; **43**: 390–403.

23 Bone RC, Balk RA, Cerra FB, *et al*. Definitions for sepsis and organ failure and guidelines for the use of innovative therapies in sepsis. The ACCP/SCCM Consensus Conference Committee. American College of Chest Physicians/ Society of Critical Care Medicine. *Chest* 1992; **101**: 1644–1655.

24 Bone RC. Sepsis and its complications: the clinical problem. *Crit Care Med* 1994; **22**: S8–S11.

25 Neumann B, Zantl N, Veihelmann A, *et al*. Mechanisms of acute inflammatory lung injury induced by abdominal sepsis. *Int Immunol* 1999; **11**: 217–227.

26 De Vooght V, Vanoirbeek JA, Haenen S, Verbeken E, Nemery B, Hoet PH. Oropharyngeal aspiration: an alternative route for challenging in a mouse model of chemical-induced asthma. *Toxicology* 2009; **259**: 84–89.

27 Ferluga J, Allison AC. Role of mononuclear infiltrating cells in pathogenesis of hepatitis. *Lancet* 1978; **2**: 610–611.

28 Nagakawa J, Hishinuma I, Hirota K, *et al*. Involvement of tumor necrosis factor-alpha in the pathogenesis of activated macrophage-mediated hepatitis in mice. *Gastroenterology* 1990; **99**: 758–765.

29 Nakayama Y, Shimizu Y, Hirano K, *et al*. CTLA-4Ig suppresses liver injury by inhibiting acquired immune responses in a mouse model of fulminant hepatitis. *Hepatology* 2005; **42**: 915–924.

30 Xiao Y, Xu J, Mao C, *et al*. 18β-Glycyrrhetinic acid ameliorates acute Propionibacterium acnes-induced liver injury through inhibition of macrophage inflammatory protein-1α. *J Biol Chem* 2010; **285**: 1128–1137.

31 Zhang Y, Cai W, Huang Q, *et al*. Mesenchymal stem cells alleviate bacteria-induced liver injury in mice by inducing regulatory dendritic cells. *Hepatology* 2014; **59**: 671–682.

32 Webert KE, Vanderzwan J, Duggan M, *et al*. Effects of inhaled nitric oxide in a rat model of Pseudomonas aeruginosa pneumonia. *Crit Care Med* 2000; **28**: 2397–2405.

33 Razavi HM, Werhun R, Scott JA, *et al*. Effects of inhaled nitric oxide in a mouse model of sepsis-induced acute lung injury. *Crit Care Med* 2002; **30**: 868–873.

34 Wang LF, Mehta S, Weicker S, *et al*. Relative contribution of hemopoietic and pulmonary parenchymal cells to lung inducible nitric oxide synthase (inos) activity in murine endotoxemia. *Biochem Biophys Res Commun* 2001; **283**: 694–699.

35 Okamoto I, Abe M, Shibata K, *et al*. Evaluating the role of inducible nitric oxide synthase using a novel and selective inducible nitric oxide synthase inhibitor in septic lung injury produced by cecal ligation and puncture. *Am J Respir Crit Care Med* 2000; **162 (2 Pt 1)**: 716–722.

36 Sittipunt C, Steinberg KP, Ruzinski JT, *et al*. Nitric oxide and nitrotyrosine in the lungs of patients with acute respiratory distress syndrome. *Am J Respir Crit Care Med* 2001; **163**: 503–510.

37 Zhu S, Ware LB, Geiser T, Matthay MA, Matalon S. Increased levels of nitrate and surfactant protein a nitration in the pulmonary edema fluid of patients with acute lung injury. *Am J Respir Crit Care Med* 2001; **163**: 166–172.

38 Ermert M, Ruppert C, Günther A, Duncker HR, Seeger W, Ermert L. Cell-specific nitric oxide synthase-isoenzyme expression and regulation in response to endotoxin in intact rat lungs. *Lab Invest* 2002; **82**: 425–441.

39 Fujii Y, Goldberg P, Hussain SN. Contribution of macrophages to pulmonary nitric oxide production in septic shock. *Am J Respir Crit Care Med* 1998; **157**: 1645–1651.

40 Szabó C. Alterations in nitric oxide production in various forms of circulatory shock. *New Horiz* 1995; **3**: 2–32.

41 Zhang L, Wang Y, Wu G, Xiong W, Gu W, Wang CY. Macrophages: friend or foe in idiopathic pulmonary fibrosis? *Respir Res* 2018; **19**: 170.

42 Wang T, El Kebir D, Blaise G. Inhaled nitric oxide in 2003: a review of its mechanisms of action. *Can J Anaesth* 2003; **50**: 839–846.

43 Tsujino I, Ushikoshi-Nakayama R, Yamazaki T, Matsumoto N, Saito I. Pulmonary activation of vitamin D. *J Clin Biochem Nutr* 2019; **65**: 245–251.

44 Piguet PF, Vesin C. Treatment by human recombinant soluble TNF receptor of pulmonary fibrosis induced by bleomycin or silica in mice. *Eur Respir J* 1994; **7**: 515–518.